Frequency-domain travel time (FDTT) measurement of ultrasonic waves by use of linear and nonlinear sources

Paul A. Johnson, Thomas M. Hopson, and Thomas J. Shankland
Earth and Environmental Sciences Division, Mail Stop D443, Los Alamos National Laboratory, Los Alamos, New Mexico 87545

(Received 10 December 1991; accepted for publication 15 July 1992)

This paper describes a frequency-domain travel time (FDTT) method for measurement of direct and reflected travel times of sound waves based on the change in phase with frequency between a reference signal and a transmitted wave. An ordinary (linear) source can be used for measuring delays over shorter path lengths, and a parametric array (nonlinear) source can be used for measuring delays over longer path lengths. In the ordinary source measurement a reference signal is electronically multiplied with a signal that is time delayed by propagation through a sample. As frequency is incremented stepwise, the relative phase difference generates a corresponding stepwise dc output from the multiplier. For any travel path within the sample, there is a characteristic period of the dc signal whose reciprocal is proportional to the group time delay along the path. If more than one arrival exists, characteristic periods are superposed. An inverse Fourier transform of the frequency signal gives the discrete arrival times for each path. In the parametric measurement, a second electronic multiplier is used to create an electronic difference frequency signal for phase comparison with a wave at the difference frequency created by nonlinear elastic interaction in the material. The FDTT method should be applicable to ultrasonic investigation of material properties, nondestructive evaluation, seismology, sonar, and architectural acoustics.

PACS numbers: 43.25.Ki, 43.25.Zx

INTRODUCTION

Numerous methods exist for laboratory measurement of ultrasonic travel time. For instance, one of the most powerful methods in use is pulse echo overlap.[1–3] This method is extremely sensitive in material where wave attenuation and scattering are low and/or propagation path lengths are short. In instances where pulse echo overlap is not possible, for example, in larger laboratory samples or highly dissipative media where only one-way wave propagation is possible, ordinary pulse methods or continuous wave methods are commonly employed.[4] Pulse methods often have the disadvantage of emergent first arriving energy making arrival time difficult to determine. In continuous-wave phase methods[4] relative phases between a reference and the detected signal can be matched precisely allowing travel time to be obtained very accurately; however, when more than one arrival is present, results from these methods can be ambiguous. Location of later arrivals in a pulsed waveform can be notoriously inaccurate, and later arrivals contaminate continuous-wave phase methods so that direct comparison between the detected signal phase and a reference signal phase may be difficult to interpret.[4] An alternative to both pulse and continuous-wave methods is use of cross correlation with a frequency swept signal as input. This method can be very powerful in obtaining direct and reflected wave travel times.

We describe an alternative method from which to obtain travel time for instances when propagation distances are relatively large and the material is highly dissipative, and/or when more than one arrival exists. The technique described here, termed the frequency domain travel time (FDTT) method, is in the general class of continuous wave methods: It relies on tracking phase differences between a reference and ultrasonic signal as a function of frequency. The FDTT method grew out of previous work in developing a frequency method by which to obtain travel time for nonlinearity created waves.[5] In this paper, we present a method than can be used to obtain travel times by using an ordinary transducer operated in the linear elastic regime. In short, the signal source is swept stepwise in frequency while the entire phase relation between the reference and detected signal is recorded in detail. Travel time can be obtained directly from the relative phase as a function of frequency. In addition, we show how the method can be employed to obtain travel times of direct and reflected waves for relatively far distances by use of a parametric array source[6] composed of two collinear, nonlinear elastic primary waves. (A parametric array is created when two collimated, high strain amplitude sound waves of different frequencies are transmitted in the same direction. The waves interact nonlinearly and create a frequency at the difference between the two primary wave frequencies.) A parametric source is useful for transmitting over large distances due to its narrow collimation and low-attenuation characteristics.[7] The linear and nonlinear sources can be used in combination for observation of direct and reflected wave travel times over a large distance interval.

Similar methods, commonly termed frequency-domain reflectometry, have been developed independently elsewhere, including in the field of optics for problems associat-

ed with optical fibers[8–10] and in ground penetrating radar for locating buried objects.[11] In addition, commercial devices that are based on the same principle exist for radar cross-sectional measurements.[12] A similar method has been applied to obtain ultrasonic travel times where the source is not stepped in frequency but swept continuously.[11] In that measurement, the multiplied signals (a reference and the phase-delayed signal propagating through the sample) are at different frequencies and the difference in frequency is directly related to the time delay. To our knowledge, however, the method described in this paper has not been applied to obtaining sonic travel times in materials, in acoustical media, or in seismic media.

I. THEORY

The basis of both the ordinary source and parametric array FDTT method rests on measuring the relative phase difference between a wave that has propagated through a sample versus a reference signal, as a function of changing frequency or wave vector. Consider a single frequency input wave $X\cos(\omega t)$ that is input into and propagates through a medium. The detected signal is composed of waves that travel directly along a path between source and detector in addition to reflected or scattered waves within the sample. For all travel paths the detected signal is of the form

$$\Psi_{\text{obs}}(\omega,t) = \sum_{i=1}^{n} A_i(\omega,L_i)B_i \cos\{\omega t - [\Phi_i(\omega) + \gamma(\omega)]\}, \tag{1}$$

where n = number of paths within the sample; $A_i(\omega,L_i)$ = frequency- and path-length-dependent attenuation coefficient; L_i = ith reflector travel path length; B_i = reflection and/or transmission coefficients, source voltage level, and transducer coupling effects to the sample; $\gamma(\omega)$ = phase shifts associated with electronics and transducers; and $\Phi_i(\omega)$ = phase delay of the ith direct or reflected wave. Note that Eq. (1) does not include frequency-dependent phase shifts due to non-normal incidence which will produce errors in time delay; however, frequency-independent phase reversal from normal incidence does not affect the time delay. Equation (1), the phase-delayed signal from the sample, is electronically multiplied with a reference signal of form

$$\Psi_{\text{ref}}(\omega,t) = A_{\text{ref}} \cos[\omega t - \gamma(\omega)]. \tag{2}$$

The reference signal is made to incorporate the same electronic phase delays $\gamma(\omega)$ as the received signal. Retaining only dc components (by filtering) yields a signal

$$V_{\text{out}}(\omega) = \frac{1}{2} A_{\text{ref}} \sum_{i=1}^{n} A_i(\omega,L_i)B_i \cos(\omega T_i), \tag{3}$$

where ωT_i is equal to $\Phi_i(\omega)$ and T_i is the ith direct or reflected wave travel time. As ω is varied, for any time delay T_i, a characteristic period results as ωT_i passes through successive values of 2π. Therefore, V_{out} represents the sum of the characteristic periods for all propagation paths L_i and their respective delay times T_i. The most expedient method by which to obtain all arrivals to inverse Fourier transform the data from the frequency domain into the time domain where each arrival is theoretically represented as a discrete spike.

A schematic illustrating the method for a single, direct arrival is shown in Fig. 1. In this, the simplest case is $n = 1$, so that the detected signal becomes

$$\Psi_{\text{obs}}(\omega,t) = A_i(\omega,L_i)B_i \cos\{\omega t - [\Phi_i(\omega) + \gamma(\omega)]\}. \tag{4}$$

Multiplication and low-pass filtering yields

$$V_{\text{out}}(\omega) = \tfrac{1}{2} A_{\text{ref}} A_i(\omega,L_i)B_i \cos(\omega T_i). \tag{5}$$

As frequency is stepped upward this function cycles at a frequency δf inversely proportional to the time delay δt of the signal traversing the sample. The actual time delay is obtained by taking the inverse Fourier transform of the resulting characteristic period signal.

A physical explanation for the representation of arrivals as spikes along the time axis comes from Fourier domain reflectometry.[8–11] Characteristic periods in the frequency domain can be considered as transforms of phase-delayed delta functions, i.e., impulse functions, in the time domain. (This behavior is analogous to an ordinary Fourier transform in which an oscillation in the time domain transforms to an impulse in the frequency domain.) Thus each arrival of travel time T_i corresponds to an impulse traveling along a particular path.

Time resolution can be enhanced by compensating for frequency-dependent attenuation of the output signal [represented by $A_i(\omega,L_i)$ above] because—within limits prescribed by signal/noise—the usable range of higher frequencies can be extended. Due to this attenuation, for a fixed

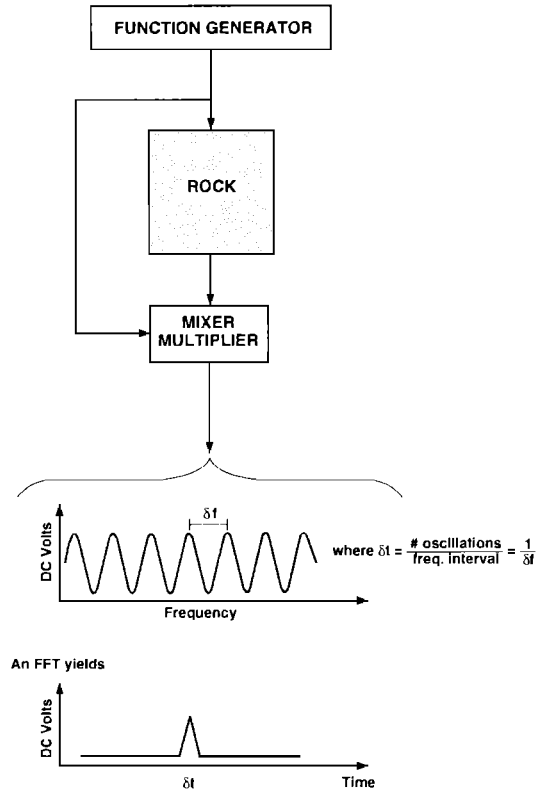

FIG. 1. Schematic diagram illustrating FDTT method.

travel distance L, the frequency-domain signal amplitude $V_{\text{out}}(\omega)$ described by Eq. (3) will decay with frequency f proportional to

$$A_L(f) \propto \exp(-\alpha L), \tag{6a}$$

where

$$\alpha L = (-\pi f/Qv),$$

L is path length, Q is specific dissipation (or quality factor), and v is wave velocity. In reality, the travel path of each reflector within the sample is of different length, which causes a different attenuation decay with frequency for each separate arrival. Nevertheless, we can make a first-order correction to remove attenuation effects and therefore increase time resolution of the inverse transform by empirically fitting a single decaying exponential to the sample output signal and then multiplying the signal by its reciprocal,

$$1/A_L(f) \propto \exp(\alpha' f), \tag{6b}$$

where $\exp(\alpha' f)$ represents the empirical fit.

In practice, care must be taken not to include significant noise in the transform. This is accomplished by inspecting the characteristic period signal and discarding the higher frequency portion where the signal/noise becomes large. Figure 2 shows an inverse Fourier transform of a measured characteristic period that has no amplitude correction (dotted line) and the same signal that was corrected before the transform was taken (solid line). Separate arrivals become much more distinct with application of the attenuation correction. [One possibility for improving the correction may be to treat each arrival independently. Instead of fitting a single decaying exponential to the frequency domain output, one approach would be to narrow-band filter the mixed output around each arrival time (corresponding to fixed characteristic period in the frequency domain), and apply the correction independently to each arrival.]

In the presence of velocity dispersion, the FDTT method gives group travel time rather than phase travel time over the frequency band of the experiment. Consider a single wave transmitted with travel time T and variable frequency ω. From Eq. (3), the mixed output signal would be

$$V_{\text{out}}(\omega) \propto \cos(\omega T) = \cos[2\pi N(\omega)], \tag{7}$$

where $N(\omega)$ represents the number of periods of the signal contained within the material. Although the material may be dispersive, if we assume the change in $N(\omega)$ over the stepped frequency band to be nearly linear in frequency, we can approximate $N(\omega)$ by a first-order Taylor series

$$N(\omega) \approx N(\omega_0) + (\omega - \omega_0)\frac{\partial N}{\partial \omega}\bigg|_{\omega=\omega_0}, \tag{8}$$

where $N(\omega_0)$ is the number of periods of the signal in the material at the starting frequency in the stepped band, and ω_0 is the starting angular frequency of the stepped frequency band. Equation (7) can then be written as

$$V_{\text{out}}(\omega) \propto \cos\left[2\pi\left(\omega \frac{\partial N}{\partial \omega}\bigg|_{\omega=\omega_0}\right) + \text{constant terms}\right]. \tag{9}$$

Therefore, as ω is increased, V_{out} will oscillate with periodicity in frequency space $(\partial N/\partial f)^{-1}$. An inverse Fourier transformation of the signal will give a travel time $T = \partial N/\partial f$ for the transmitted signal.

By definition, group velocity U is

$$U = \frac{\partial \omega}{\partial k} = \frac{2\pi}{\partial k/\partial f}. \tag{10}$$

Letting

$$k = 2\pi/\lambda = 2\pi N/L, \tag{11}$$

where L is the fixed travel length of the wave, we then have

$$\frac{\partial k}{\partial f} = \left(\frac{2\pi}{L}\right)\left(\frac{\partial N}{\partial f}\right). \tag{12}$$

Therefore,

$$U = \frac{L}{\partial N/\partial f} = \frac{L}{T_{\text{group}}}, \tag{13}$$

where T_{group} is group time delay. Therefore,

$$T_{\text{group}} = \frac{L}{U} = \frac{\partial N}{\partial f}. \tag{14}$$

This is the same expression derived for $T = \partial N/\partial f$ from Eq. (9) above.

A more intuitive way to perceive that group travel time is measured by the FDTT method is to consider each arrival as an impulse. Because the impulse must be synthesized from the band of frequencies propagating through the medium, its arrival must occur at the group travel time of the band. The peak amplitude on the time axis marks the arrival of the energy maximum for a given travel path.

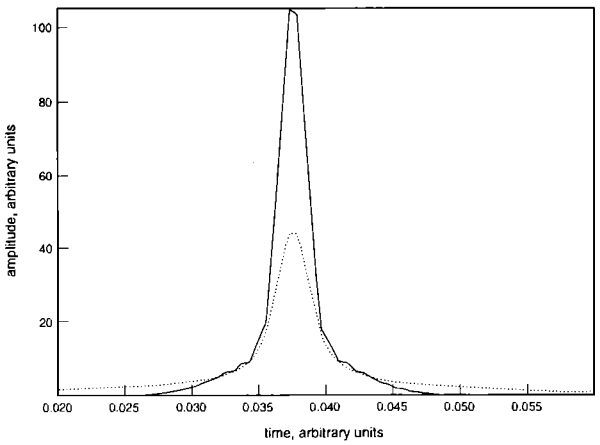

FIG. 2. Synthetic, time domain representation of the frequency-domain signal without attenuation compensation (dotted line) and with attenuation compensation (solid line). One percent random noise was included in the frequency-domain signal. The time-domain signals were smoothed before plotting.

II. EXPERIMENTAL METHOD AND APPARATUS

This section describes the experimental apparatus for both the ordinary source and parametric array measurements. Figure 3 shows a block diagram of the experimental apparatus for measuring travel times in the linear, ordinary source case. The signals are generated by an HP 8904 A

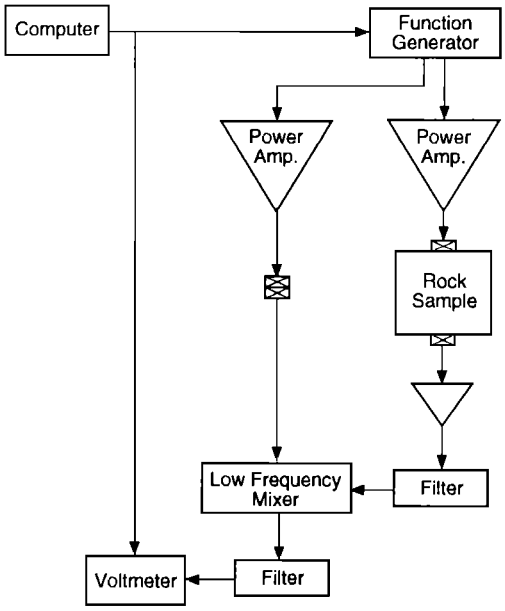

FIG. 3. FDTT method experimental configuration for an ordinary, linear elastic source.

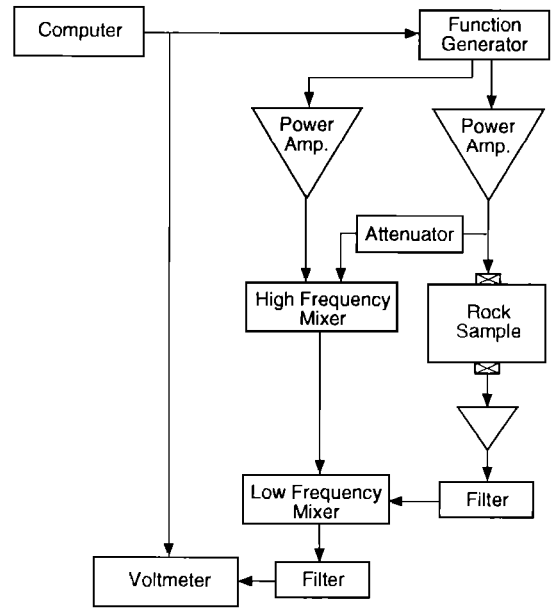

FIG. 4. FDTT method experimental configuration for a parametric array (nonlinear elastic) source.

synthesizer whose two phase-locked output signals are identical except in amplitude: A large amplitude signal is directed via an ENI A-300 power amplifier to the rock and a small amplitude signal is directed through an identical amplifier to the mixer. The source and receiver are identical Panametrics 2.54-cm-diam PZT transducers. The output signal is preamplified by a Tektronix AM 502 differential amplifier with a 10-kHz-1-MHz bandpass and is directed to a mixer[5] where it is multiplied with the reference signal. In order to compensate for phase delays induced by the electronics, the reference signal passes through identical electronics before multiplication (excluding the preamplifier, which induces negligible phase shift over the band of input frequencies used). The mixer low-pass filters at 2 Hz leaving only the difference frequency signal at dc. The mixer output is sampled by an HP 3457 A multimeter that averages the signal over the time of one power line cycle to diminish incoherent noise. The multimeter output is proportional to the signal amplitude and the cosine of the phase difference between this signal and the reference signal as in Eq. (3). Frequency is stepped rather than swept to allow for the time delay across the sample and for time averaging in the multimeter. At each frequency step the time-averaged value is read and stored by an IBM AT computer that also controls the experiment. The duration of a complete measurement depends on several factors, including propagation dimension, desired signal/noise from the multimeter, desired time resolution, and maximum travel time measured after inverse Fourier transformation. However, a complete measurement generally takes between 10–40 min.

Figure 4 shows the experimental configuration for the parametric array measurement. In this case, the synthesizer generates two separate signals summed into a single output that is directed into the rock through the power amplifier. Another output, lower in voltage and consisting of only one of the primary frequencies f_1 or f_2, is directed through a power amplifier into a high-frequency mixer–multiplier.[5] The other input into the high-frequency mixer comes from the amplified signal before being routed to the rock and consists of primary frequencies $f_1 + f_2$ (the attenuator, used to protect the mixer, induces negligible phase delay). The high-frequency mixer creates an electronic difference frequency signal at $f_1 - f_2$ (in addition to other, undesirable frequencies that are filtered by the mixer), while the rock creates an elastic wave difference frequency signal from nonlinear wave-mixing. The preamplified signal from the rock is multiplied at the low-frequency mixer–multiplier with the electronically derived difference frequency signal created by the high-frequency mixer. Again, the dc voltage out of the first mixer is proportional to the difference-frequency signal amplitude and to the cosine of the relative phase difference. Phase delays induced by the transducers are not accounted for because of the limitation imposed by the low-frequency mixer on a minimum input level. Measurements show that there can be up to a 0.6-μs delay due to the transducers (a second preamplifier would alleviate this problem). Otherwise, the measurement is identical to the ordinary source case.

III. RESULTS

In the first part of this section we present results from two single (linear) source measurements to obtain direct transmission travel time in a rectangular solid sample of Berea sandstone with dimensions of 1829 mm(x), 453 mm(y), and 458(z), respectively, as shown in Fig. 5. Measurements were carried out along the x- and y dimensions of the sample as shown in the figure. A velocity anisotropy of approximately 13% exists between these two directions due to preferred orientation of cracks and grains along bedding planes

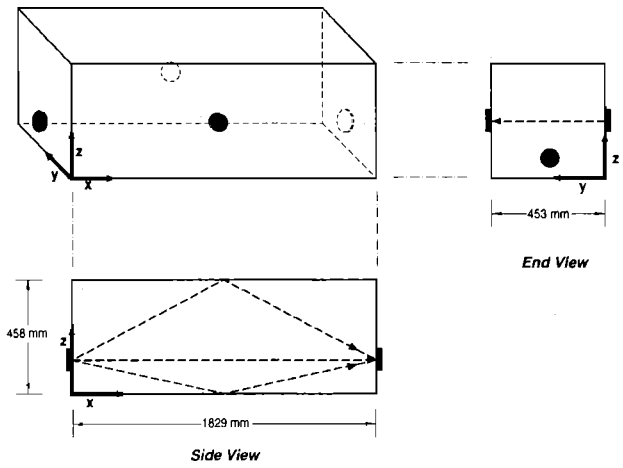

FIG. 5. Schematic of rock sample illustrating sample dimensions, locations of transducers (solid discs), and ray paths (dashed lines).

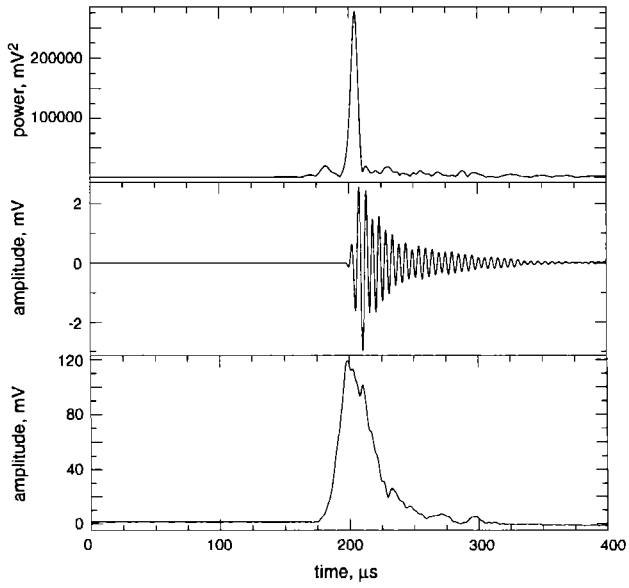

FIG. 7. (a) (top) Inverse Fourier transform of Fig. 6 showing time of arrival (peak). (b) (center) Measured pulse across identical path. (c) (bottom) Smoothed, absolute value of the cross correlation from a frequency swept signal obtained from the identical path.

in the x-z dimension (2.22 mm/μs in the y direction and 2.56 mm/μs in the z direction). In the second part we show measurements from a reflector, in this case the back wall of the sample, in order to compare the single source and parametric array measurements and to demonstrate that the FDTT method is appropriate for reflection uses.

Figure 6 shows the attenuation corrected, frequency domain characteristic period for the 453-mm-long path length (y dimension) in the rock sample using a single input stepped from 50 to 670 kHz at frequency intervals of 100 Hz. The gradual growth of the signal between 50 and 250 kHz arises from the combined frequency response characteristics of the 1-MHz transducers and the bandlimited 0.3–35-MHz power amplifiers. Figure 7(a) shows the inverse Fourier transform of this signal and, for comparison, Fig. 7(b) and (c) show pulse-mode and cross-correlation results for the same path. In Fig. 7(b), a single sine wave cycle input at 600 kHz that was summation averaged for the same duration as the FDTT observation (approximately 30 min) so that the total energies are comparable. Figure 7(c) is the smoothed, absolute value of the cross correlation of a signal swept over the identical frequency interval as the FDTT measurement. As for the pulsed measurement the swept signal was collected over the same duration as the FDTT measurement so that energies are comparable. The signal from the function generator was used as the reference in the correlation and a Hamming window was applied before correlation.

In Fig. 7(a), the peak of the transformed signal, located at approximately 204 μs, lags the emergent pulsed arrival in Fig. 7(b) by roughly 4 μs; however, the main energy of the pulsed arrival is slightly delayed with respect to the FDTT signal. The delay time obtained from the correlation signal peak is early, approximately 198 μs, and the correlation signal/noise is lower. In addition, the correlation signal peak is broader than the peak obtained using the FDTT method. The differences in travel times will be addressed in the discussion section. Note the superior signal/noise obtained in using the FDTT method.

Figure 8 shows the attenuation corrected, frequency-domain signal for paths along the 1829-mm-long x dimension of the sample using an ordinary source signal stepped from 100 to 360 kHz at intervals of 100 Hz. Source and receiver transducers were centered at 12 cm from the sample bottom, well away from the sample center in the x–z plane, so that all side-wall reflections could be recorded. As a result, the frequency-domain signal envelope seen in Fig. 8 is more complicated than in the previous case because it includes reflected arrivals. Figure 9(a) shows the inverse Fourier transform of this signal. Figure 9(b) shows a pulse arrival of a single sine wave cycle input at 600 kHz that was transmitted over the same signal path and summation averaged over the same duration as the FDTT method (approximately 30 min). The first arrival in Fig. 9(a) occurs at approximately 714 μs, while the arrival time of the emergent

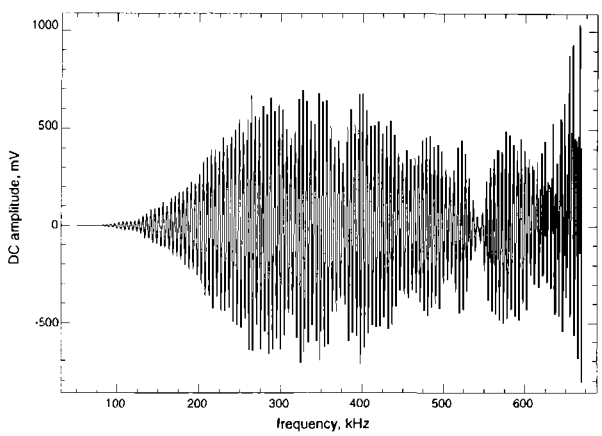

FIG. 6. Attenuation compensated, characteristic period for 453-mm path.

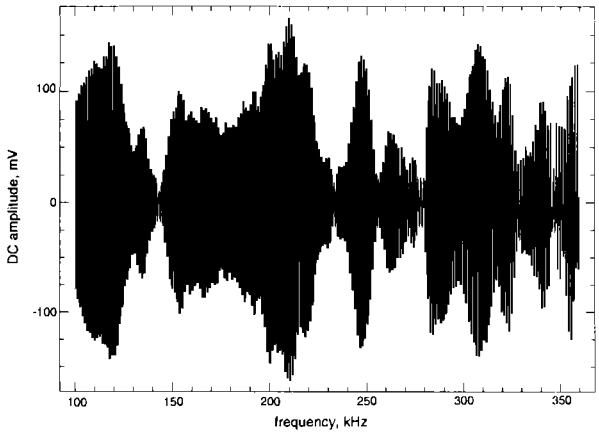

FIG. 8. Attenuation corrected, frequency-domain signal from 916-mm dimension (linear, ordinary source case).

pulse appears to be at approximately 718 μs. Later arrivals in Fig. 9(a) correspond to bottom-wall (x–y plane), side-wall (x–z plane), and top-wall (x–y plane) reflectors. Of these, the side-wall reflector is the largest amplitude arrival at approximately 777 μs because the two side-wall reflectors have identical path lengths from source to receiver and therefore arrive simultaneously. The second arrival at 727 μs may be the bottom reflector. (We have not corrected for the frequency-dependent phase lag produced by non-normal incidence reflection. Therefore, those arrivals will be somewhat in error.)

Figure 10(a) shows the frequency-domain signal for an ordinary (linear) source stepped from 100 to 400 kHz at

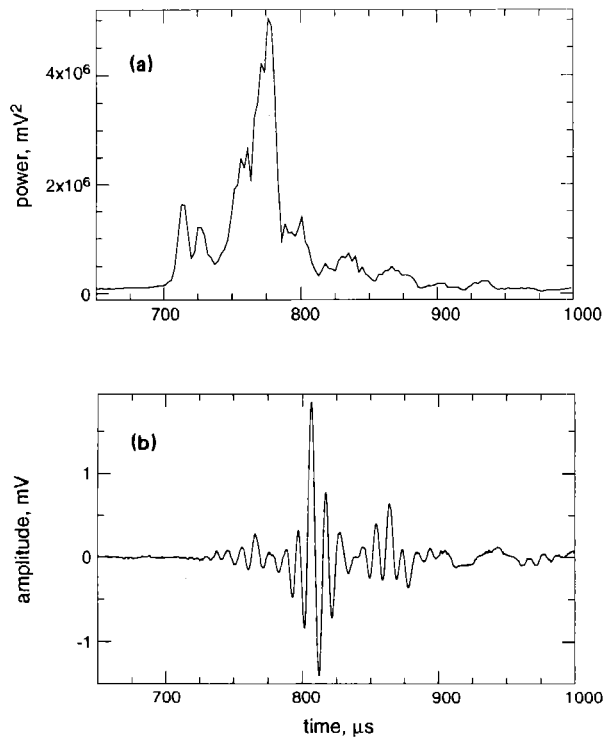

FIG. 9. (a) (top) Inverse Fourier transform of Fig. 8. (b) (bottom) Measured pulsed arrival across 1828-mm dimension.

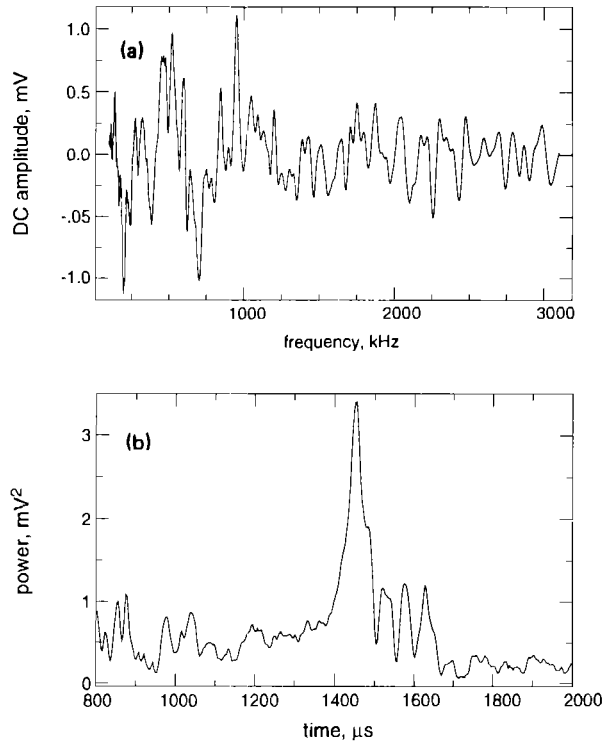

FIG. 10. (a) (top) Attenuation corrected, frequency-domain reflected signal from 2×1829-mm dimension (linear, ordinary source case). (b) (bottom) Inverse Fourier transform of (a).

intervals of 100 Hz in which source and receiver transducers were placed side-by-side to detect the signal reflected from the back wall. The measurement was made lengthwise down the 1829-mm x dimension and therefore the total travel path was 3658 mm. Again, the signal is composed of more than one arrival, the direct surface wave seen as the low-frequency characteristic period that dominates the frequency-domain signal, and the back-wall reflector that is shorter in characteristic period. The latter is best seen in the early part of the frequency-domain signal. The inverse Fourier transformed signal is seen in Fig. 10(b) expanded around the predicted travel time (1428 μs) of the direct arrival from the back-wall reflector. Other arrivals correspond to side-wall and corner reflections; however, it is not clear which peak corresponds to a given reflection. No pulsed arrival was observable in this case, a demonstration of the signal/noise advantage of working in the frequency domain. The direct surface wave between adjacent transducers was the largest amplitude arrival in this case; however, it is an early arrival and does not appear in the time window of Fig. 10(b).

Figure 11(a) shows a parametric array result in which the side-by-side transducer configuration was once again used. In this case, one primary was stepped from 100 to 400 kHz, while the other primary was held fixed at 250 kHz. Figure 11(b) shows the corresponding transformed signal. As with the preceding ordinary source measurement, the reflected first arrival time falls at 1454 μs but the peak is narrower, possibly due to the reduction of sidelobes in the difference frequency signal radiation pattern. (Note that the phase delay of the transducers, up to 0.6 μs, is not accounted

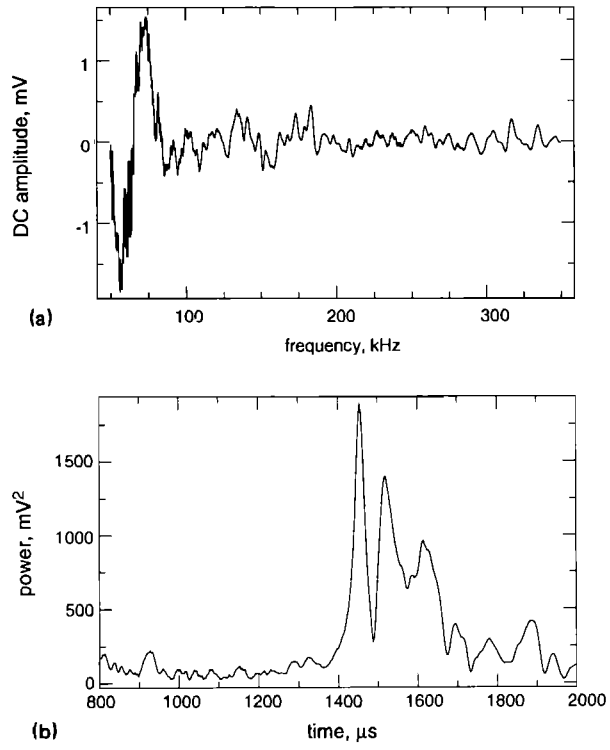

FIG. 11. (a) (top) Attenuation corrected, frequency-domain reflected signal from 2×1829-mm dimension (parametric array case). (b) (bottom) Inverse Fourier transform of (a).

for.) The following two arrivals do not correspond to the predicted arrivals from the side-wall and top-wall reflectors, nor do they correspond to the later peaks observed in the ordinary source case; however, the addition of strong back-reflected energy from sample corners, the effects of path-dependent attenuation, and the lower frequency band of the parametric array case make comparison difficult. Note the signal/noise is nearly six times that of the ordinary source case. Again, the direct surface wave arrival does not appear in the time window, and no pulsed arrival was detected.

IV. DISCUSSION

In this section, several discrepancies in the observations between methods will be addressed. This will be followed by considerations when applying the FDTT method. In addition, it will be shown that phase reversals from normal incidence, important in geophysical applications, can be inferred from the FDTT method.

A. Observed discrepancies

Differences in travel times between methods used for comparison to the FDTT method (pulse and cross correlation) are shown for the 453-mm path length [Fig. 7(a)–(c)]. The difference of several μs in the first arrival obtained using the FDTT method, in contrast to the pulsed first arrival, is due to velocity (and possibly path) dispersion. The abrupt step at the beginning and end of the input waveform give rise to broadband energy that propagates at frequency-dependent velocities in a dispersive medium. Thus the group delay measured in the case of the pulse is that of the first arriving energy; however, in the FDTT method, out of all frequencies that may be present in the detected signal at a given frequency step, *only* the detected signal at the reference frequency is multiplied in the mixer. In effect, the mixer is a notch filter. Therefore, the group delay of the specified frequency band is obtained, not necessarily the group delay of the first arriving energy. The arrival time obtained by use of cross correlation is somewhat ambiguous. If the peak value of the envelope is used, the arrival is early at approximately 198 μs. If the center of the envelope is used, it corresponds reasonably well with the arrival time obtained by the FDTT method.

B. Application considerations

Because the measurement is carried out over a frequency band determined by desired time resolution and overall delay time (to be discussed), an accurate measurement requires that the group velocity of the material must also be reasonably constant over this frequency interval. This will generally be the case for high-Q (low-attenuation) materials. Media with significant velocity dispersion over the frequency interval of data collection will smear the travel time peak in the transformed data because the characteristic period will change as a function of driving frequency. Where travel time is large as in the case of large samples, the period will be high so that there will be sufficient periods in a relatively short swept band to perform a transform. Hence, dispersion effects can be ignored and smearing effects will be small if the dispersion itself is small over the frequency interval required by the measurement. Conversely, for short travel times and therefore large bandwidths in a dispersive medium, the method may not perform well because of arrival time smearing.

There are trade-offs between the total frequency span, frequency sampling rate (the frequency step interval), and aliasing. The frequency interval dictates the maximum travel time after inverse Fourier transformation through the Nyquist criterion; smaller frequency steps increase the time interval upon transformation. If arrivals exist that are not contained in the time interval, aliasing will appear. A well-known property of digital data is that there is no possibility of applying an antialias filter as can be done for analog data. There is no other way to alleviate this problem other than to be certain that the time interval is long enough for all arrivals to appear. Although long travel times can be a problem where severe reverberations exist, they can be less important in rocks because of attenuation. Note also that expanding the total frequency span and/or decreasing the frequency sampling interval increases the measurement time.

Optical frequency-domain reflectometry and radar imaging methods were mentioned in the Introduction as conceptually identical to the FDTT method. In contrast to the method described here, these techniques also employ an additional quadrature (imaginary component) measurement in conducting the phase comparison. Once the in-phase and quadrature signals have been obtained, they are combined to generate separate phase and amplitude data as a

function of frequency. An inverse Fourier transform is then performed on the data to obtain travel time information of the various reflectors within the material. Although not necessary to the measurement, the quadrature phase comparison provides an additional independent measurement at a given frequency that improves signal/noise ratio. Measuring both in-phase and quadrature signals is especially convenient when a lock-in amplifier is available.

Part of the motivation for developing a parametric array source is to make use of the high-collimation, low-frequency (and, therefore, low-attenuation) characteristics of the array. The improvement in signal/noise by use of the parametrically generated difference signal over the ordinary source signal is approximately six times for this example owing to lower attenuation at the inherently lower frequency compared to the primary frequencies. Although there is a tradeoff between conversion efficiency versus narrow collimation,[13] the benefits of using a parametric array are clear when distances of wave propagation are far, at least in rock[14] and other highly attenuating, nonlinear materials.

C. Phase considerations

Phase information can be important, for instance in seismology where phase shifts at reflections indicate acoustic impedance contrasts diagnostic of material at the interface. This is a frequent consideration in hydrocarbon exploration. Figure 12 shows the result of using a synthetic characteristic period containing two travel times [$n = 2$ in Eq. (1)] in which arbitrary phases of 0 and $\pi/2$ were included in the cosine argument, and in which both in-phase and quadrature signals are included. As seen in Fig. 13 the FDTT method can recover the starting phases along with the travel times. Work in this area is continuing.

V. CONCLUSIONS

The FDTT method is used for measuring direct and reflected ultrasonic wave travel times in which arrivals are readily picked out as if they were transmitted or reflected impulses. The method relies on measurement of the phase difference between a reference signal and a signal that has propagated through a sample. The phase difference is recorded over an interval of driving frequency. Recording the entire phase curve allows the signal to be inverse Fourier transformed, thus providing separation and determination of travel time for each discrete arrival within the sample. A nonlinearly created difference frequency beam was also used, the benefit being enhanced signal/noise over large propagation distances. Coupled together, the frequency-domain method using both an ordinary (linear) source and a parametrically derived source provides a travel time measurement tool useful over various sample lengths. The FDTT method should have numerous applications in acoustics, ultrasonics, seismology, and nondestructive evaluation where sharp time resolution and identification are required.

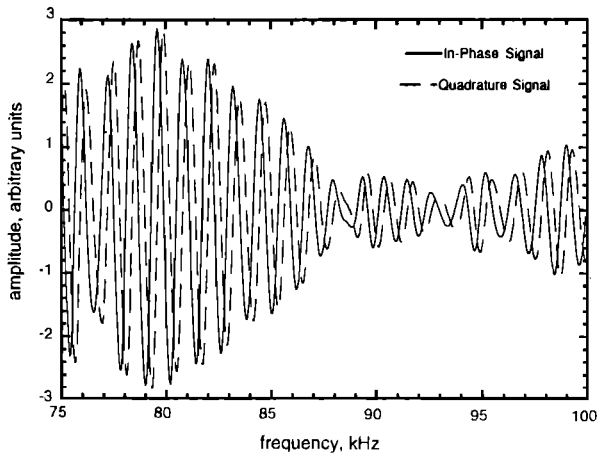

FIG. 12. Synthetic representation of in-phase and quadrature signals.

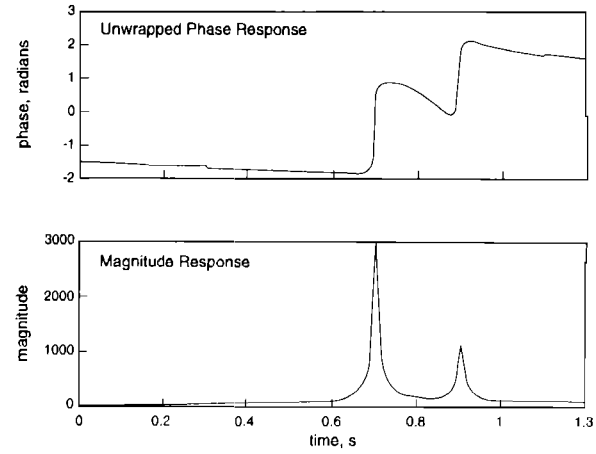

FIG. 13. Unwrapped phase (top) and magnitude (bottom) of Fig. 12.

ACKNOWLEDGMENTS

This work was supported by the Office of Basic Energy Science of the U.S. Department of Energy under Contract W-7405-ENG-36 with Los Alamos National Laboratory. We thank Albert Migliori for suggesting the fundamental concept behind this work. We also thank R. J. O'Connell, Peter Roberts, Michael Fehler, Christoph Borel, Leigh House, Scott Phillips, Brian Bonner, Katherine McCall, Doug Meegan, and Greg Eischeid for helpful discussions, and Steve Taylor for careful review of the manuscript.

[1]J. E. May, "Precise measurement of time delay," IRE Natl. Conv. Rec. **6**, 134 (1958).

[2]E. P. Papadakis, "Ultrasonic phase velocity by the pulse-echo overlap method incorporating phase corrections," J. Acoust. Soc. Am. **44**, 1437 (1964).

[3]J. Toulouse and C. Launay, "Automated system for relative sound velocity and ultrasonic attenuation measurements," Rev. Sci. Instrum. **59**, 492–495 (1988).

[4]E. P. Papadakis, "Ultrasonic velocity and attenuation: Measurement methods with scientific and industrial applications," in *Physical Acoustics*, edited by W. P. Mason and R. N. Thurston (Academic, New York, 1976), Vol. XII, Chap. 5, pp. 315–318.

[5]P. A. Johnson, T. J. Shankland, and A. M. Migliori, "Continuous wave phase detection for probing nonlinear elastic wave interactions in rocks," J. Acoust. Soc. Am. **89**, 598–603 (1991).

[6]P. J. Westervelt, "Parametric acoustic array," J. Acoust. Soc. Am. **26**, 535–537 (1963).

[7]T. G. Muir, "Nonlinear acoutics: A new dimension in underwater sound," in *Science, Technology and the Modern Navy, 30th Anniversary 1946–1976*, edited by E. I. Salkovitz (Department of the Navy, Office of Naval Research, Arlington, VA, 1976), pp. 548–569.
[8]H. Ghafoori-Shiraz and T. Okoshi, "Fault location in optical fibers using optical frequency domain reflectometry," J. Lightwave Tech. **LT-4**, 316–322 (1986).
[9]M. Shadaram and R. Hippenstiel, "Fourier analysis of the complex envelope of the echos in an OFDR," Appl. Opt. **25**, 1083–1085 (1986).
[10]H. Vanhamme, "High resolution frequency-domain reflectometry," IEEE Trans. Instrum. Meas. **39**, 369–375 (1990).
[11]K. Iizuka and A. P. Freundorder, "Detection of nonmetallic buried objects by a step frequency radar," Proc. IEEE **71**, 276–279 (1983).
[12]Hewlett Packard, "Radar cross-section measurements with the HP 8510 network analyzer," Product Note No. 8510-2.
[13]J. L. S. Bellin and R. T. Beyer, "Experimental investigation of an end-fire array," J. Acoust. Soc. Am. **34**, 1051–1059 (1962).
[14]P. A. Johnson, T. J. Shankland, R. J. O'Connell, and J. N. Albright, "Nonlinear generation of elastic waves in crystalline rock," J. Geophys. Res. **92**, 3597–3602 (1987).